CellPress
PARTNER JOURNAL

Molecular Plant
Research Article

Progressive Regulation of Sesquiterpene Biosynthesis in *Arabidopsis* and Patchouli (*Pogostemon cablin*) by the miR156-Targeted SPL Transcription Factors

Zong-Xia Yu[1,2,3,4], Ling-Jian Wang[2], Bo Zhao[2,3], Chun-Min Shan[2,3], Yu-Hua Zhang[5], Dong-Fang Chen[5] and Xiao-Ya Chen[1,2,*]

[1]Plant Science Research Center, Shanghai Chenshan Botanical Garden, Shanghai Key Laboratory of Plant Functional Genomics and Resources, Shanghai 201602, China

[2]National Key Laboratory of Plant Molecular Genetics, National Plant Gene Research Center, Institute of Plant Physiology and Ecology, Shanghai Institutes for Biological Sciences, Chinese Academy of Sciences, Shanghai 200032, China

[3]University of CAS, Beijing 100049, China

[4]College of Bioengineering, Dalian University, Dalian 116622, China

[5]Firmenich Aromatics (China) Co. Ltd., Shanghai 201108, China

***Correspondence: Xiao-Ya Chen (xychen@sibs.ac.cn)**

http://dx.doi.org/10.1016/j.molp.2014.11.002

ABSTRACT

Plant metabolites vary at different stages of their life cycle. Although it is well documented that environmental factors stimulate biosynthesis of secondary metabolites, the regulation by endogenous developmental cues remains poorly understood. The microRNA156 (miR156)-targeted SQUAMOSA PROMOTER BINDING PROTEIN-LIKE (SPL) factors function as a major age cue in regulating developmental phase transition and flowering. We show here that the miR156-targeted SPL transcription factor plays an important role in the spatiotemporal regulation of sesquiterpene biosynthesis. In *Arabidopsis thaliana*, the miR156-SPL module regulates the formation of (*E*)-β-caryophyllene in the flowering stage through modulating expression of the sesquiterpene synthase gene *TPS21*. We demonstrated that SPL9 directly binds to *TPS21* promoter and activates its expression. In the perennial fragrant herb *Pogostemon cablin*, the accumulation of patchouli oil, largely composed of sesquiterpenes dominated by (−)-patchoulol, is also age-regulated, and the SPL promotes biosynthesis of sesquiterpenes in elder plants by upregulating patchoulol synthase (*PatPTS*) gene expression. As miR156-SPLs are highly conserved in plants, our finding not only uncovers a molecular link between developmental timing and sesquiterpene production but also suggests a new strategy to engineer plants for accelerated growth with enhanced production of terpenoids.

Key words: miR156 targeted SPLs, *TPS21*, *PatPTS*, sesquiterpene biosynthesis, *Pogostemon cablin*, *Arabidopsis*

Yu Z.-X., Wang L.-J., Zhao B., Shan C.-M., Zhang Y.-H., Chen D.-F., and Chen X.-Y. (2015). Progressive Regulation of Sesquiterpene Biosynthesis in *Arabidopsis* and Patchouli (*Pogostemon cablin*) by the miR156-Targeted SPL Transcription Factors. Mol. Plant. **8**, 98–110.

INTRODUCTION

Plants produce copious low molecular weight organic compounds known as specialized or secondary metabolites, of which terpenoids form the largest and most diversified group (Pichersky and Gang, 2000; Falara and Pichersky, 2012). During sesquiterpene biosynthesis, the C5 isoprene units of isopentenyl diphosphate (IPP) and its isomer dimethylallyl diphosphate (DMAPP) are produced by the cytosolic mevalonate (MVA), then prenyltransferases catalyze the condensation of DMAPP with IPP to form farnesyl diphosphate (FPP), which is converted by terpene synthases (TPSs) into sesquiterpenes (C15), most of

Published by the Molecular Plant Shanghai Editorial Office in association with Cell Press, an imprint of Elsevier Inc., on behalf of CSPB and IPPE, SIBS, CAS.

which are cyclic. These compounds can be further modified by reactions such as oxidation, dehydrogenation, and acylation, resulting in the great diversity of sesquiterpenoid products (Bohlmann et al., 1998; Newman and Chappell, 1999; Dudareva et al., 2004). TPSs are of central importance because they not only direct the isoprenoid flux into specific groups of metabolites but also determine the basic skeletons of the products and, thus, the final terpenome (Christianson, 2008; Degenhardt et al., 2009; Tholl and Lee, 2011).

Plant terpenoids have many physiological and ecological functions, such as serving as phytoalexins in defense against pests and pathogens, and signals in biocommunications and interactions, and thus contribute greatly to plant survival and successful reproduction in a natural ecosystem (Kessler and Baldwin, 2001; Pichersky and Gershenzon, 2002; Engelberth et al., 2004; Maffei et al., 2011). In addition, plant terpenoids also possess great commercial value, as some terpenoids are widely used as flavorings, fragrances, and pharmaceuticals; this has stimulated many attempts to increase their yield in plants (Goff and Klee, 2006; Li and Vederas, 2009). Patchouli (*Pogostemon cablin*), a perennial herbaceous species of the mint family (Lamiaceae or Labiatae), is a commercial fragrant plant that produces patchouli oil, which is distinct for primarily consisting of sesquiterpenes, with (−)-patchoulol as the dominant constituent (Deguerry et al., 2006). Five sesquiterpene synthases from patchouli have been identified, of which four converted FPP into one major product: PatTpsA for γ-curcumene, PatTpsCF2 for (+)-germacrene A, and both PatTpsBF2 and PatTpsB15 for (−)-germacrene D. The last (and also the pivotal) product, patchoulol synthase (PatPTS, PatTps177), is a multiproduct sesquiterpene synthase responsible for the production of most components of patchouli oil, including patchoulol and at least 13 other sesquiterpenes (Deguerry et al., 2006).

Many investigations have focused on the regulation of terpenoid biosynthesis related to stress signals. However, production and accumulation of secondary metabolites in plants are often organ- or tissue-specific, and their amounts and compositions change during plant development and aging (Facchini and De Luca, 1995; Gershenzon et al., 2000). For example, in peppermint (*Mentha* × *piperita* L.), monoterpenes are present in peltate glandular trichomes instead of capitate ones, and accumulate rapidly in the first 21 days of early leaf development, then level off and sustain a relatively stable level during the rest of leaf life (Gershenzon et al., 2000; Turner et al., 2000). In snapdragon (*Antirrhinum majus*), the components of floral scent, including myrcene, ocimene, and methylbenzoate, are primarily released from the upper and lower petal lobes of the flower; the emissions increase rapidly on the second day after anthesis and reach maximum at the sixth day, followed by decline thereafter (Dudareva et al., 2003). These reports imply that the biosynthesis of terpenoids in plant is subjected to developmental stage regulation.

Arabidopsis thaliana has similar features of terpene biosynthesis and emission. After flowering, a blend of terpenes are released from the inflorescence, with (*E*)-β-caryophyllene as the predominant constituent (Aharoni et al., 2003; Chen et al., 2003). There are 32 *TPS* genes in the *Arabidopsis* genome (Aubourg et al., 2002), among which two sesquiterpene synthases, *TPS21* and *TPS11*, are responsible for the vast majority of floral sesquiterpenes (Tholl et al., 2005). TPS21 catalyzes the conversion of FPP into (*E*)-β-caryophyllene plus minor amounts of α-humulene and α-copaene, and TPS11 is responsible for the formation of essentially all of the remaining floral sesquiterpenes including (+)-thujopsene (Aharoni et al., 2003; Chen et al., 2003; Tholl et al., 2005). Both *TPS11* and *TPS21* genes are predominantly expressed in flowers; *TPS11* is expressed in nectaries and ovules, whereas *TPS21* is highly expressed in stigma but moderately in sepals and anther filaments (Chen et al., 2003; Tholl et al., 2005). It has been reported that the AUXIN RESPONSE FACTOR 6 (ARF6) and ARF8 trigger the expression of two jasmonic acid (JA)-inducible genes, *MYB21* and *MYB24*, by enhancing JA production, which in turn promote petal, stamen, gynoecium, and nectary development and consequently affect sesquiterpene production (Mandaokar et al., 2006; Reeves et al., 2012), indicating that biosynthesis of sesquiterpenes in flowers is related to floral organ development and flower maturation. Nonetheless, to date a direct molecular link between plant development and terpene biosynthesis is lacking.

In plants, miR156, an evolutionary highly conserved microRNA (miRNA), plays a key regulatory role in both vegetative phase transition and flowering through targeting a subset of transcription factors named SQUAMOSA PROMOTER BINDING PROTEIN-LIKE (SPL) (Wang et al., 2009; Wu et al., 2009; Yamaguchi et al., 2009; Huijser and Schmid, 2011). In addition, SPLs participate in controlling fertility (Xing et al., 2010; Xing et al., 2013), embryo development (Nodine and Bartel, 2010), cell size (Wang et al., 2008; Usami et al., 2009), leaf initiation rate (Schwarz et al., 2008; Wang et al., 2008), and trichome distribution (Shikata et al., 2009; Yu et al., 2010). Besides these developmental aspects, the miR156-targeted SPLs are also connected to the biosynthesis of phenylpropanoids, as SPL9 was shown to repress anthocyanin accumulation by destabilizing the MYB-bHLH-WD40 transcriptional activation complex (Gou et al., 2011).

Serving as an endogenous age cue for timing plant development, miR156 levels off gradually after germination, leading to increased levels of the targeted SPLs during plant growth and development (Axtell and Bartel, 2005; Wang et al., 2009; Wu et al., 2009). Here, we report that the progressive biosynthesis of (*E*)-β-caryophyllene in *Arabidopsis* inflorescence after flowering is regulated by miR156-targeted SPLs, which directly activate *TPS21* expression. We further show that in the perennial herb patchouli, a similar regulatory mechanism is functioning: the SPL regulates both patchouli oil production and vegetative phase transition.

RESULTS

Arabidopsis TPS21 Expression Changes with miR156 Level

After flowering, *Arabidopsis* inflorescences emit a range of volatiles, of which 60% are terpenes, mostly sesquiterpenes (Aharoni et al., 2003; Chen et al., 2003). Several *TPS* genes, including *TPS03*, *TPS14*, and *TPS24*, as well as the two well-characterized sesquiterpene synthase genes, *TPS11* and *TPS21*, were found to be highly or preferentially expressed in

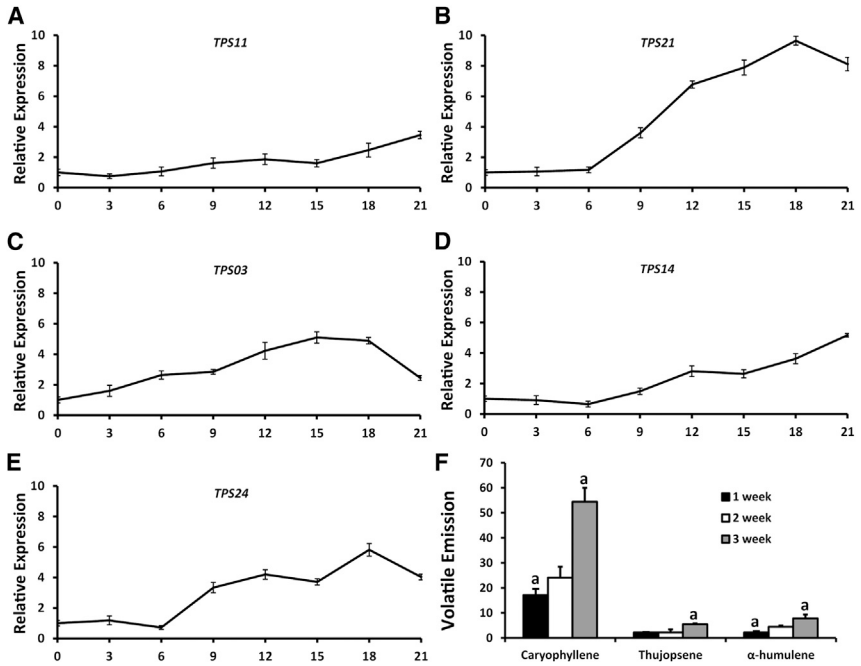

Figure 1. Progressive Upregulation of *TPS* Genes and Sesquiterpene Emissions.

(A–E) The expression levels of *TPS11* **(A)**, *TPS21* **(B)**, *TPS03* **(C)**, *TPS14* **(D)**, and *TPS24* **(E)** in inflorescences of different ages (the inflorescences were collected at different days after flowering, and the day of bolting is indicated as 0 on the *x* axis). The level in inflorescences of day 0 was set to 1. Error bars indicate the SD of three biological replicates.

(F) Emissions of (*E*)-β-caryophyllene, (+)-thujopsene, and α-humulene from the wild-type inflorescences of different ages (ng/g fresh weight [FW] and hour [ng/g FW·h]). The inflorescences were collected at different weeks after bolting. Error bars indicate the SD of three biological replicates. Student's *t*-test, $^{a}P < 0.01$. The statistically significant differences between 1-week-old and 2-week-old inflorescences, and between 2-week-old and 3-week-old inflorescences, are calculated.

flowers (Chen et al., 2003; Hong et al., 2012). To further examine their temporal expression patterns, we collected the inflorescences on different days after flowering (DAF) and conducted quantitative real-time PCR (qRT-PCR). We found that, in general, transcript levels of the five *TPS* genes were increasing in developing flowers (Figure 1A–1E). In particular, *TPS21* exhibited the most striking enhancement of expression, reaching the maximum level at 18 DAF (Figure 1A–1E). Because TPS11 and TPS21 are responsible for producing most sesquiterpenes, which constitute 95% of *Arabidopsis* floral terpene volatiles, we chose them for further investigation. Consistent with previous results, gas chromatography–mass spectrometry (GC–MS) analysis showed that the floral emissions of TPS21 products, (*E*)-β-caryophyllene and α-humulene, were elevated after flowering (Figure 1F). The increased release was also observed for (+)-thujopsene (Figure 1F), albeit to a lesser extent.

Since miR156-targeted SPLs function in promoting the vegetative-to-reproductive transition and flowering, we asked whether they were involved in regulating terpene biosynthesis in inflorescence. First, we detected the volatiles from inflorescences of transgenic plants overexpressing miR156 (*Pro35S:MIR156*) or a mimicry form of miR156 (*Pro35S:MIM156*) that elevates the level of SPLs (Franco-Zorrilla et al., 2007). The amount of (*E*)-β-caryophyllene, a dominant sesquiterpene component, was substantially increased in *Pro35S:MIM156* but drastically reduced in *Pro35S:MIR156* floral emissions, compared with those of the wild-type (Figure 2A and Supplemental Figure 1), indicating that miR156 indeed played a role in regulating terpene biosynthesis. The amount of (+)-thujopsene released, however, remained little changed in either the *Pro35S:MIM156* or *Pro35S:MIR156* emissions (Figure 2A).

To uncover how miR156 controls *Arabidopsis* sesquiterpene biosynthesis, we analyzed the expression of genes of the sesquiterpene biosynthetic pathway. In plant cells, FPP, a common precursor of sesquiterpenes, is derived from the MVA pathway (Newman and Chappell, 1999). The *Arabidopsis* genome contains two HMG-CoA reductase (HMGR) genes, *HMGR1* and *HMGR2*, which catalyze the formation of mevalonate, and two farnesyl diphosphate synthase (FPS) genes, *FPS1* and *FPS2* (Enjuto et al., 1994; Cunillera et al., 2000). Analysis with qRT-PCR showed that none of these MVA pathway genes were obviously affected by changes in the level of miR156 (Figure 2B), suggesting the possibility that the downstream *TPS* genes could serve as targets of SPLs.

As reported, *TPS11* and *TPS21* are predominantly expressed in inflorescence, with (+)-thujopsene and (*E*)-β-caryophyllene as their major products, respectively (Tholl et al., 2005). Consistent with the great variation in (*E*)-β-caryophyllene emission (Figure 2A), the *TPS21* expression level was increased by more than two-fold in *Pro35S:MIM156* but drastically reduced in *Pro35S:MIR156* inflorescences (Figure 2C). For *TPS11*, neither its expression nor the product emission was significantly affected by miR156 (Figure 2A and 2C).

We then extended the analysis to other *TPS* genes. We found that the expression levels of *TPS14* and *TPS24* were also affected by miR156-SPLs, but the effect was not clear for *TPS03* and two other putative *TPS* genes, *TPS17* and *TPS18* (Supplemental Figure 2), whose function has not been identified. These data indicate that miR156 affects a subset of *TPS* genes, with a profound effect on *TPS21* and its product, which dominates *Arabidopsis* floral volatiles. Notably, among the *TPS* genes examined, *TPS21* also exhibited the most clear age-dependent temporal expression pattern in inflorescence (Figure 1A–1E).

Correlated Expression Patterns of *TPS21* and *SPL9*

In *A. thaliana*, 11 of the 17 *SPL* genes are targeted by miR156 and can be divided into four clades: SPL3/4/5, SPL9/15, SPL2/10/11, and SPL6/13A/B (Guo et al., 2008). We then detected the *TPS21* expression level in transgenic plants expressing the

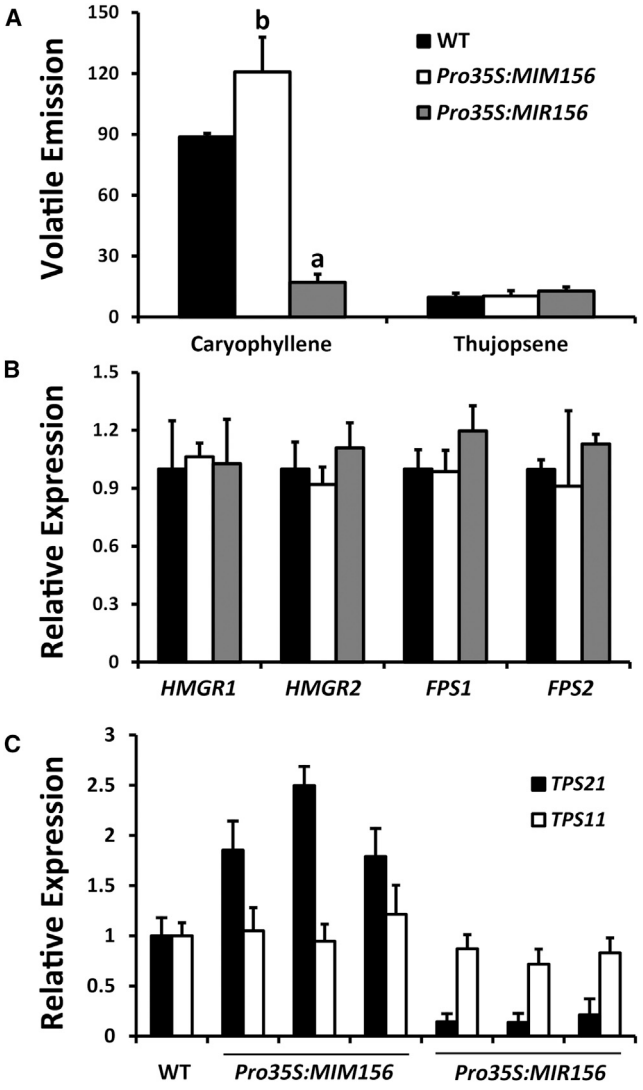

Figure 2. Effects of miR156 on *Arabidopsis* Sesquiterpene Biosynthesis.

(A) Emissions of (*E*)-β-caryophyllene and (+)-thujopsene from the wild-type (WT), *Pro35S:MIM156*, and *Pro35S:MIR156* inflorescences (ng/g FW·h) at 3 weeks after bolting. Error bars indicate the SD of three biological replicates. Student's *t*-test, $^{a}P < 0.01$ and $^{b}P < 0.05$.

(B) qRT-PCR analysis of the expression levels of the MVA pathway genes of *HMGR1, HMGR2*, *FPS1*, and *FPS2* in inflorescences. The level in the wild-type was set to 1. Error bars indicate the SD of three biological replicates.

(C) qRT-PCR analysis of *TPS21* and *TPS11* expression levels in inflorescences. Error bars indicate the SD of three biological replicates.

miR156-resistant form of *SPL* genes (*rSPLs*), *Pro35S:rSPL3*, *ProSPL9:rSPL9*, and *Pro35S:rSPL10*. Compared with that of the wild-type, *TPS21* expression was elevated in all transgenic lines, although to different degrees (Figure 3A). Among the three SPLs tested, SPL9 was most effective in promoting *TPS21* expression, which was then chosen for further investigation.

To dissect the molecular link between *TPS21* and the miR156-targeted SPLs, represented here by *SPL9*, we first compared their spatial expression patterns in both vegetative and reproductive organs. We found that *SPL9* had the highest level of transcripts in inflorescence and a moderate level in stem and silique; similarly, *TPS21* transcripts were most abundant in inflorescence (Figure 3B). As reported previously, in stems *SPL9* is expressed in an acropetal manner, with the highest level at the top and the lowest in the junction between the stem and rosette leaves (Yu et al., 2010; Gou et al., 2011). *TPS21* exhibited the same expression pattern as *SPL9*, with a gradual increase of transcript abundance along the stem from the bottom up (Figure 3C).

To further examine the regulation of *TPS21* expression by SPLs, we employed the transgenic plants that expressed a dexamethasone (DEX)-inducible form of *rSPL9* (*ProSPL9:rSPL9-GR*), or an ethanol-inducible miR156 (*ProAlcA:MIR156*). Application of DEX to the *ProSPL9:rSPL9-GR* plants doubled the *TPS21* expression (Figure 3D). By contrast, when *ProAlcA:MIR156* plants were treated with 5% ethanol, whereby transient overproduction of miR156 would cause the decline of the *SPL* levels, *TPS21* expression was decreased by 50% (Figure 3D). Next, we introduced a *GUS* reporter gene driven by the *TPS21* promoter into *Pro35S:MIM156* or *Pro35S:MIR156* plants, respectively. β-Glucuronidase (GUS) staining was pronouncedly enhanced in *Pro35S:MIM156* but barely visible in *Pro35S:MIR156* inflorescences, compared with that in the wild-type (Figure 3E–3G), suggesting that the SPLs might target the *TPS21* promoter *in vivo*.

SPL9 Directly Binds To and Activates *TPS21* Promoter

The GTAC motif has been identified as the core binding site of SPLs (Klein et al., 1996; Birkenbihl et al., 2005; Kropat et al., 2005; Liang et al., 2008). Within a 1376-bp fragment of the *TPS21* gene upstream of the translation start codon, there are eight GTAC motifs (Figure 4A). To assess whether SPL9 could bind to these *cis*-regulatory motifs, an electrophoretic mobility shift assay (EMSA) was performed using a recombinant HIS-SPL9 protein. The 1376-bp fragment was divided into three segments, designated cis1, cis2, and cis3, with an approximately 70-bp overlap between them (Figure 4A). SPL9 showed a strong binding capacity to cis1, moderate binding to cis3, and weak, if any, binding to cis2 (Figure 4B). The specificity of this binding was confirmed in a competition assay with excess amounts of unlabeled probes of cis1 and cis3, respectively (Figure 4B). One of the possible explanations for the discrepancy among these *cis* elements is that the adjunct nucleotides around the GTAC motif could influence the SPL–DNA interaction.

We then investigated the binding capability of SPL9 to *TPS21* promoter *in vivo*. A chromatin immunoprecipitation (ChIP) assay was performed using the *ProSPL9:GFP-rSPL9* transgenic plants, in which *rSPL9* was fused in-frame to the green fluorescent protein (GFP) coding region. Four genomic fragments spanning all eight GTAC motifs, namely I, II, III, and IV (Figure 4A), were examined, among which fragments I, II, and IV, but not III, were apparently enriched to varying degrees after pull-down with an anti-GFP antibody (Figure 4C). In accordance with the EMSA results, the affinity between SPL9 and cis1 (consisting of fragments I and II) was the highest, followed by cis3 (consisting

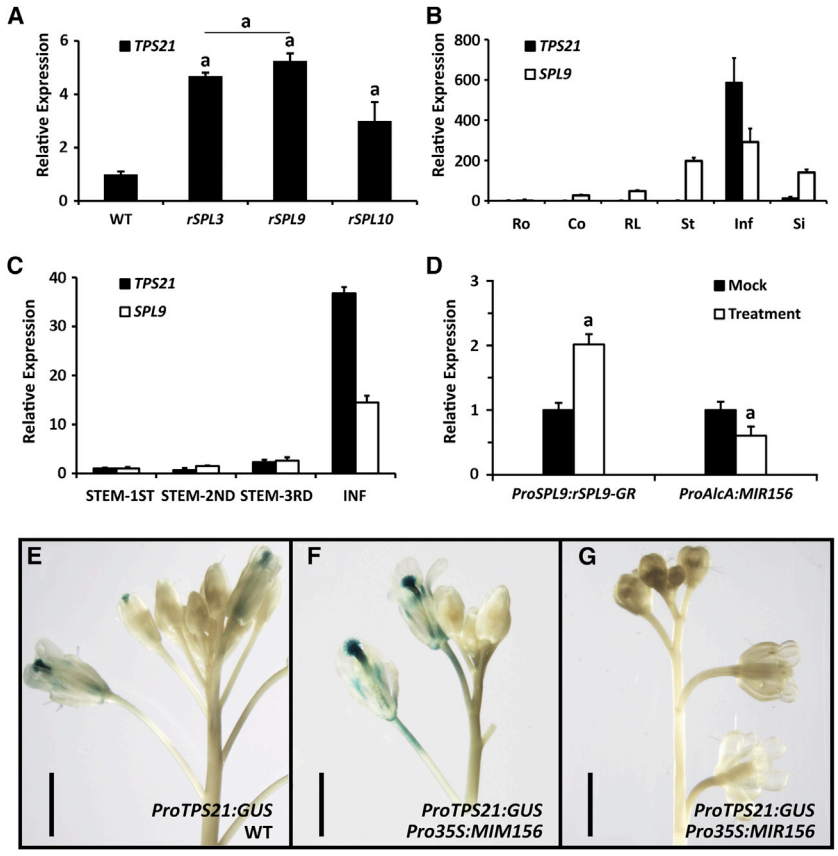

Figure 3. Expression of *TPS21* Is Regulated by miR156-Targeted *SPL*s.

(A) Transcript levels of *TPS21* in inflorescences of the wild-type (WT), *Pro35S:rSPL3* (*rSPL3*), *ProSPL9:rSPL9* (*rSPL9*), and *Pro35S:rSPL10* (*rSPL10*) plants, analyzed by qRT-PCR. The level in the wild-type was set to 1. Error bars indicate the SD of three biological replicates. Student's *t*-test, $^{a}P < 0.01$. The statistically significant differences between wild-type and different *rSPL* transgenic plants (*rSPL3*, *rSPL9*, or *rSPL10*), and between *rSPL9* and *rSPL3*, are calculated.

(B) qRT-PCR analysis of transcript levels of *TPS21* and *SPL9* in root (Ro), cotyledon (Co), rosette leaf (RL), stem (St), inflorescence (Inf), and silique (Si) of *Arabidopsis* as indicated. The levels of *TPS21* and *SPL9* in root were set to 1. The 1-week-old seedlings were used for the root and cotyledon analysis and 1-month-old plants were used for the remaining tissues. Error bars indicate the SD of three biological replicates.

(C) Spatial expression patterns of *TPS21* and *SPL9* in the main stem and inflorescences of wild-type *Arabidopsis*. 1st to 3rd represent three successive internodes of the main stem from the bottom up. The levels of *TPS21* and *SPL9* in the first internode of the main stem were both set to 1. Error bars indicate the SD of three biological replicates.

(D) Transient expression of *TPS21* in *ProSPL9:rSPL9-GR* rosette leaves (before bolting) after DEX **(left)** treatment and in *ProAlcA:MIR156* inflorescences after ethanol **(right)** treatment. Values from *ProSPL9:rSPL9-GR* plants treated with DMSO and *ProAlcA:MIR156* with water were set to 1 and used as control. Error bars indicate the SD of three biological replicates. Student's *t*-test, $^{a}P < 0.01$.

(E–G) GUS staining assay of *TPS21* promoter activity in wild-type **(E)**, *Pro35S:MIM156* **(F)**, and *Pro35S:MIR156* **(G)** inflorescences. Bar, 1 cm.

of fragment IV). These data indicate that SPL9 binds directly to the promoter of *TPS21* both *in vitro* and *in vivo*.

To determine whether the SPL binding motifs were required for *TPS21* promoter activity, we constructed five mutant versions of *TPS21* promoter: in *mu1* the six upstream GTAC motifs were deleted, in *mu2* and *mu3* the respective GTAC motif was changed to AAGA, *mu2+3* was a double mutant containing both cis2 and cis3 mutations, and finally the six upstream motifs in *mu2+3* were deleted to form *mu4*, which contained no intact GTAC motif at all (Figure 5A). The intact (*INT*) and different mutant versions of the *TPS21* promoter were fused to the firefly luciferase (LUC) reporter gene, and the promoter activities were then detected by using a transient dual-LUC assay system in *Nicotiana benthamiana* (Liu et al., 2008). Compared with the mock control, the LUC activity of *INT* was greatly increased when cotransformed with *Pro35S:rSPL9* (Figure 5B), indicating that SPL9 activated *TPS21* expression. The *mu1* and *mu4* mutations seriously impaired this activation, and *mu3* and *mu2+3* compromised it to a different extent, whereas the *mu2* mutation did not exhibit any effect (Figure 5B). Similar results were obtained with transgenic plants harboring the *GUS* reporter gene driven by the *TPS21* promoter and its mutant versions. GUS staining showed a moderate decrease in inflorescence for the *mu2+3* promoter, and a great reduction for the *mu1* and *mu4* promoters (Figure 5C–5F). Thus, data from both transient dual-LUC and stable transformation GUS assays demonstrate that the GTAC motifs, particularly those located in cis1, are responsible for transcriptional activation of the *TPS21* promoter by SPL9.

As *mu2+3* and *mu1* disrupted *TPS21* promoter activities to a different extent, we introduced them into *Pro35S:MIM156* and *Pro35S:MIR156* plants, respectively. GUS staining of the inflorescence showed that the *mu2+3* promoter activity was enhanced in *Pro35S:MIM156* but attenuated in *Pro35S:MIR156* backgrounds (Figure 5G and 5H), suggesting that the *cis* elements outside the region of *mu2+3* (cis2 and cis3) operated well for SPL-mediated *TPS21* promoter activation, which was further supported by the fact that the GUS staining of *mu1* remained undetectable even in the *Pro35S:MIM156* background (Figure 5I and 5J). Therefore, the six upstream GTAC motifs in cis1 are crucial for transcriptional activation of *TPS21* by SPL9.

SPLs Regulate Sesquiterpene Abundance

As SPLs, in particular SPL9, positively regulate *TPS21* transcription, we determined the amount of sesquiterpene components released from inflorescences of the transgenic plants with different levels of SPL9. The *ProSPL9:rSPL9* plants exhibited a phenotype similar to that of *Pro35S:MIM156* with skipped juvenile phase and earlier flowering, whereas the *spl9* homozygous

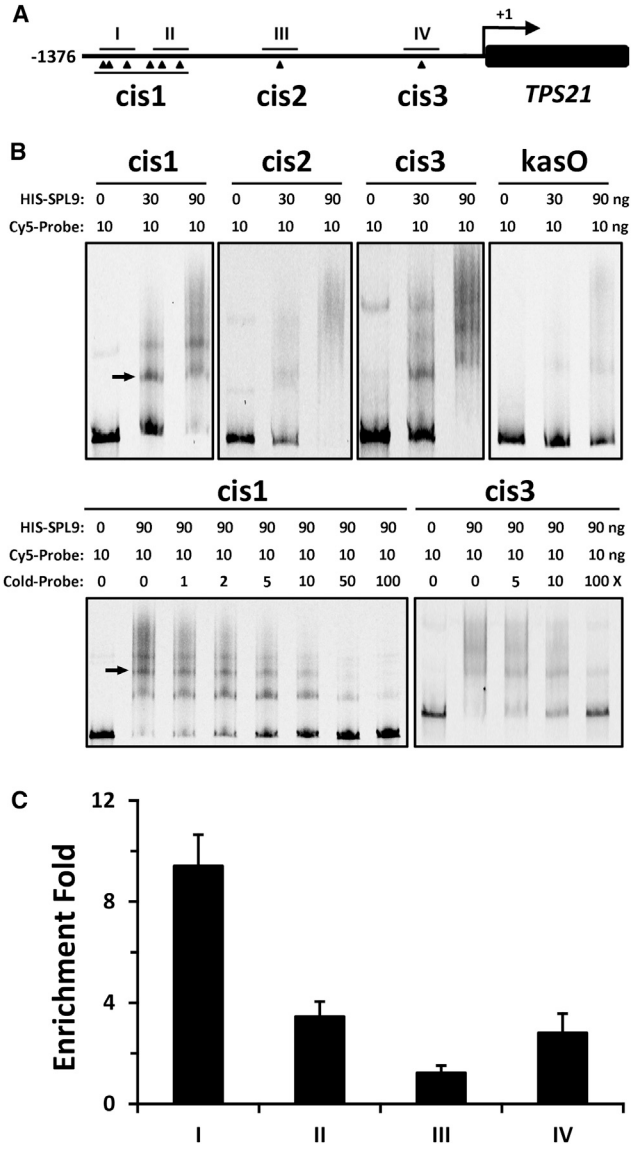

Figure 4. SPL9 Binds to *TPS21* Promoter.

(A) Diagram of *TPS21* promoter region. Solid triangles represent GTAC elements in the *TPS21* promoter region, which was divided into three segments (cis1, cis2, and cis3) with ~70 bp nucleotides overlapping between each other, and used in the EMSA assay; I–IV represent the DNA fragments used in ChIP analysis (see below). The black box indicates the *TPS21* coding region.

(B) EMSA assay of SPL9 binding ability to *TPS21* promoter. Ten nanograms of Cy5-labeled cis1, cis2, and cis3 fragments were incubated with different concentrations of HIS-SPL9 fusion protein (0, 30, and 90 ng) **(upper)**; the *kasO* promoter fragment of *Streptomyces coelicolor* was used as a negative control. Then the labeled cis1 and cis3 were incubated with 90 ng HIS-SPL9 to compete with different concentrations of cold probes of cis1 (0, 0, 1, 2, 5, 10, 50, 100×) and cis3 (0, 0, 5, 10, 100×), respectively **(lower)**. The specific bands are indicated with a solid arrow.

(C) ChIP enrichments of *TPS21* promoter regions bound by GFP-SPL9. Inflorescences of the 4-week-old *ProSPL9:GFP-rSPL9* and the wild-type plants were used, and DNA fragments were analyzed by qRT-PCR with the *β-TUBULIN2* promoter as a reference. Enrichment of each fragment was referred to the *ProSPL9:GFP-rSPL9* against wild-type plants. Error bars indicate the SD of three separate samples.

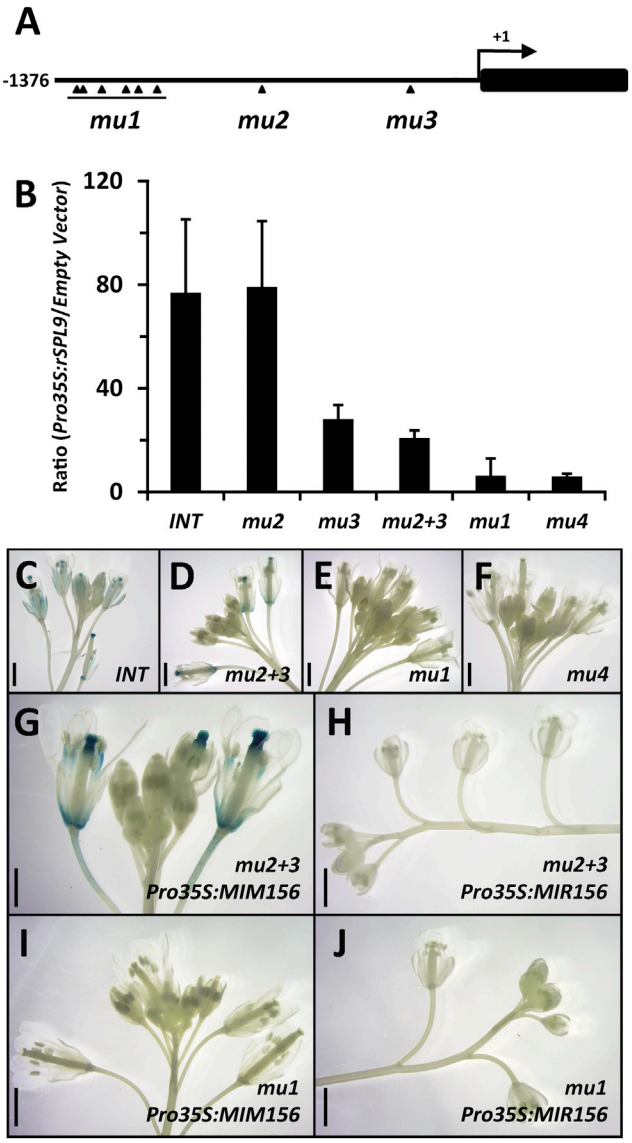

Figure 5. SPL Binding Sites are Required for *TPS21* Promoter Activity.

(A) The eight GTAC boxes in the *TPS21* promoter region were deleted or mutated, shown as *mu1*, *mu2*, and *mu3*, and the black box indicates reporter genes (*GUS* or *LUC*). For details of promoter mutation, see the Methods section.

(B) Relative activity of SPL9 on the intact and mutant versions of *TPS21* promoter in transiently transformed *N. benthamiana* leaves. Both the intact (*INT*) and the mutant versions of *TPS21* promoter were fused to *LUC* reporter. The relative LUC activities were first normalized to REN, and the ratio (LUC/REN) of the samples cotransformed with *Pro35S:rSPL9* was compared with that of *Empty Vector*. Error bars indicate the SD of three biological replicates.

(C–F) GUS staining of inflorescences. *GUS* reporter was driven by the intact (*INT*) and mutant (*mu1*, *mu2+3*, *mu4*) *TPS21* promoter, respectively. Bar, 2 mm.

(G–J) GUS staining of inflorescences showing the *mu2+3* and *mu1* promoter activity in *Pro35S:MIM156* **(left)** and *Pro35S:MIR156* **(right)** backgrounds. Bar, 2 mm.

mutant (T-DNA insertion, SAIL_150_B05) showed a slight delay in flowering and an increase in branching. The transcript level of *TPS21* was elevated to approximately 2.5-fold in *ProSPL9:rSPL9*

and dropped to less than 50% in *spl9*, whereas the *TPS11* expression was largely unaffected (Supplemental Figure 3A). Consistent with gene expression, (*E*)-β-caryophyllene content was elevated by 76% in the *ProSPL9:rSPL9* but halved in the *spl9* mutant emissions, compared with the wild-type. The amount of TPS11 products emitted, represented by (+)-thujopsene, was much less affected than (*E*)-β-caryophyllene and remained low for both transgenic lines (Supplemental Figure 3B). It is clear that SPL9 plays an important role in regulating *TPS21* gene expression and, consequently, the biosynthesis and emission of (*E*)-β-caryophyllene. Since the *TPS21* expression level was decreased to a greater degree in *Pro35S:MIR156* than in *spl9* (Figure 2C and Supplemental Figure 3A), and SPL3 and SPL10 also promoted *TPS21* expression (Figure 3A), these miR156-controlled SPLs may function additively in regulating *TPS21* expression.

SPLs Regulate *TPS21* Expression in Parallel with MYC2

Our previous investigation demonstrated that MYC2 directly up-regulates *TPS21* and *TPS11* expression in *Arabidopsis*, and the amount of (*E*)-β-caryophyllene released from inflorescences of two T-DNA insertion mutants of MYC2, *myc2-1* and *myc2-2*, was decreased to about one-half of that of the wild-type (Hong et al., 2012). To determine whether MYC2 was involved in SPL-mediated activation of *TPS21*, a mutant *ProTPS21:GUS* harboring an invalid MYC2 binding site (*ProTPS21 E-box mu2:GUS*) in the wild-type and an original *ProTPS21:GUS* in the *myc2-2* mutant plants were transformed with *Pro35S:MIM156* and *Pro35S:MIR156*, respectively. The GUS staining in inflorescence was faint when the second MYC2 binding motif in the *TPS21* promoter was mutated or in the *myc2-2* mutant background, as previously reported (Hong et al., 2012), but *Pro35S:MIM156* and *Pro35S:MIR156* still upregulated or downregulated the *TPS21* promoter activity, respectively (Figure 6). These data suggest that both SPLs and MYC2 are involved in regulating *TPS21* expression in inflorescence, and that they function independently.

Patchouli Oil Content and *PatPTS* Expression Mount with Age

Patchouli accumulates considerable essential oil, which consists of over 24 different sesquiterpenes instead of a blend of diversified compounds (Buré and Sellier, 2004). The major constituent, (−)-patchoulol, takes approximately 35% of the total amount (Deguerry et al., 2006).

We analyzed the content of patchouli oil in leaves collected at different stages of growth. GC–MS showed that in leaf extracts, patchoulol content increased along with plant aging (Figure 7A). Patchoulol was undetectable in juvenile plants (1–2 weeks old) and became evident in one-month-old plants, although its level was still low. Afterwards, the amount of patchoulol elevated markedly, and reached as much as about 12-fold higher in one-year-old plants in comparison with that in the one-month-old plant (Figure 7A). Consistently, the expression level of *PatPTS* was rising drastically with plant aging (Figure 7B). Although the patchouli oil content in young leaves might be underestimated due to the higher water content, the greater than 10-fold increase in the amount of oil in the 1-year-old leaf and the temporal pattern of *PatPTS* gene expression clearly suggest a link between patchoulol accumulation and age-regulated *TPS* gene expression.

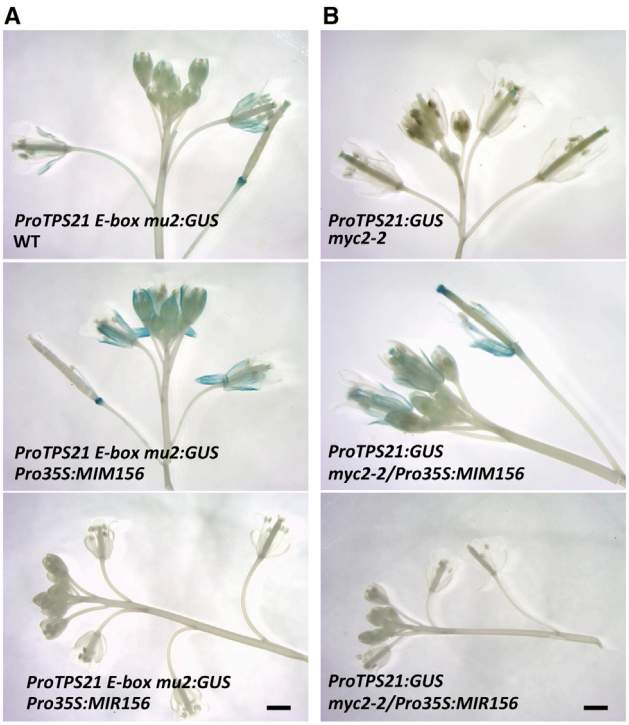

Figure 6. SPLs and MYC2 Regulate *TPS21* Expression in Parallel.

(A) GUS staining showing activity of the mutant *TPS21* promoter (one E-box was mutated, referred to as *ProTPS21 E-box mu2:GUS*) in the wild-type (WT), *Pro35S:MIM156*, and *Pro35S:MIR156* backgrounds. Bar, 2 mm.

(B) GUS staining of the intact *TPS21* promoter activity in *myc2-2*, *myc2-2/Pro35S:MIM156*, and *myc2-2/Pro35S:MIR156* backgrounds. Bar, 2 mm.

SPLs Regulate Sesquiterpene Biosynthesis in Patchouli

Given that in *Arabidopsis* SPL9 directly regulates *TPS21* expression and biosynthesis of the predominant sesquiterpene component (*E*)-β-caryophyllene, we asked whether SPLs also regulated sesquiterpene biosynthesis in patchouli. Because overexpressing *rSPL9* (*Pro35S:rSPL9*) could cause plant sterility (Wang et al., 2008), *SPL10* (*Pro35S:rSPL10*) was chosen for patchouli transformation.

Analysis of the 10-month-old plant showed that, in comparison with the control, the *PatPTS* transcript level was increased up to five-fold in *Pro35S:rSPL10* leaves, but decreased to a very low level in *Pro35S:MIR156* (Figure 8A). Consistently, PatPTS products were substantially elevated in *Pro35S:rSPL10* leaf extracts (Table 1). The content of the major product, (−)-patchoulol, was elevated by 20% in *Pro35S:rSPL10*; by striking contrast, it was below the detectable level in *Pro35S:MIR156* (Figure 8B and 8C). We then extended qRT-PCR analysis to all five sesquiterpene synthase genes identified from patchouli (Deguerry et al., 2006), of which *PatPTS* showed a much higher expression level than others in leaf, and *PatTpsBF2* expression seemed also affected by miR156 and rSPL10 (Supplemental Figure 4). These data indicate that

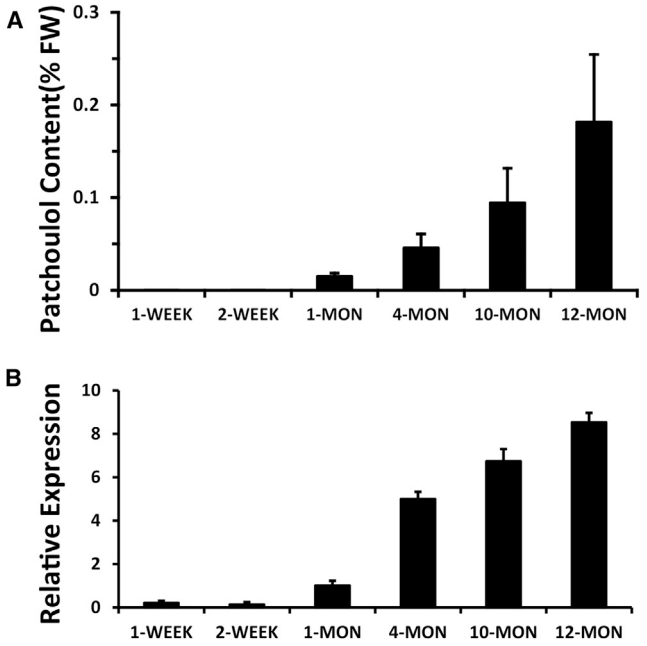

Figure 7. Content of Patchoulol, a Major Constituent of Patchoulol Oil, and *PatPTS* Expression in Patchouli Leaf from Plants of Different Ages.

(A) Contents of patchoulol in patchouli leaf of different ages. The amount of (−)-patchoulol was calculated by comparing with the internal standard and then dividing by the FW of the sample. Error bars indicate the SD of three biological replicates.

(B) qRT-PCR analysis of *PatPTS* transcript level in leaves. The second fully expanded leaf (from the top) was chosen. Error bars indicate the SD of three biological replicates.

PatPTS, the predominant sesquiterpene synthase gene responsible for patchouli oil biosynthesis, is under the control of miR156-targeted SPLs.

Leaves of these transgenic lines were then regenerated to produce rejuvenescent plants by tissue culture. In leaves of the 1-month-old regenerated lines of *Pro35S:rSPL10*, *PatPTS* expression was elevated obviously, as well as the (−)-patchoulol content (Figure 8D and 8E). *PatPTS* expression and (−)-patchoulol content were sharply decreased in *Pro35S:MIR156* (Figure 8D and 8E). These results demonstrate that the miR156-targeted SPLs upregulate the *PatPTS* expression and patchouli oil biosynthesis in the perennial herb patchouli.

DISCUSSION

Secondary metabolites contribute greatly to plant adaptation to unpredictable environments and successful reproduction (Pichersky and Gershenzon, 2002; Falara and Pichersky, 2012). These small organic compounds can be produced instantly in plant cells in response to external stimuli, during which phytohormones, such as JA, are the major mediators in transmitting the induction signals (Memelink et al., 2001; Balbi and Devoto, 2008). On the other hand, secondary metabolites are often synthesized and stored in specific structures or tissues of defined organs, and the metabolite profile varies along with plant growth and development (Bouwmeester et al., 1998; Turner et al., 2000; Chen et al., 2003; Dudareva et al., 2003; Tholl and Lee, 2011); in this regard, the secondary metabolism in plants must be well coordinated with the growth and development.

We have demonstrated that in *A. thaliana*, the miR156-targeted SPLs show a direct and strong regulation on *TPS21*, which is responsible for the biosynthesis of (*E*)-β-caryophyllene, a predominant component of the sesquiterpene volatiles released from flowers. We also found that miR156-SPLs play a similar role in patchouli in promoting the expression of *PatPTS* and the production of patchouli oil. *PatPTS* is a predominant sesquiterpene synthase gene of patchouli with regard to its expression level in leaf and its critical role in the biosynthesis of patchouli oil. Thus, in both species, the sesquiterpene synthase selected by miR156-targeted SPLs becomes the dominant enzyme in producing sesquiterpenes, at least at a defined developmental stage. We propose that the miR156-controlled SPLs play an important role in determining the formation and composition of terpenoids in each plant species by recruiting and substantially upregulating specific members of the *TPS* gene family, thus contributing to the chemical identity of the plant.

Arabidopsis is thought to be a self-pollinated plant; however, distinct genomic recombinations exist among accessions of different origin (Stahl et al., 1999; Kuittinen and Aguade, 2000; Haubold et al., 2002). The observation that flowers are occasionally visited by insects in the wild (Hoffmann et al., 2003), which may cause pollen transfer between populations, provides a good explanation for the genomic recombination. The emitted terpenes may serve as an olfactory cue to attract pollinators. As the rates of cross-pollination are low, floral volatiles may have other functions. For example, the major sesquiterpene of *Arabidopsis* floral volatiles, (*E*)-β-caryophyllene, is active in directly inhibiting bacterial growth on the sigma (Huang et al., 2012). Although to date there have been no comprehensive investigations on the role of patchoulol in plant biotic or abiotic defense, it could serve as an antimicrobial reagent and insect deterrent (Wu et al., 2006; Zaim et al., 2013). In any case, the involvement of miR156-SPLs in regulating the developmental biosynthesis of terpenoid confers much to the successful reproduction of the plant population (Wu et al., 2006; Huang et al., 2012; Zaim et al., 2013).

Besides *TPS21*, a subset of *TPS* genes of *Arabidopsis* are progressively upregulated in inflorescence with plant age. A plausible explanation is that, in addition to miR156 targeted SPLs, other transcription factors also participate in the regulation of sesquiterpene biosynthesis. As we illustrated for *Arabidopsis*, both the JA signaling pathway transcription factor MYC2 and the miR156-targeted SPLs are involved in regulating terpene biosynthesis in flowers, and act on *TPS21* gene expression in parallel. In *Artemisia annua*, both AaWRKY1 and AaERFs promote artemisinin biosynthesis by activating *ADS* expression (Ma et al., 2009; Yu et al., 2012b). Moreover, in tobacco NtMYC2 controls nicotine biosynthesis by directly targeting *putrescine N-methyltransferase 2* (*PMT2*) and *quinolinate phosphoribosyltransferase 2* (*QPT2*) genes, or indirectly by upregulating the *NIC2*-locus *ERF* genes, which then activate *PMT2* and *QPT2* expression (Shoji and Hashimoto, 2011; Zhang et al., 2012). Thus, it is a common feature that

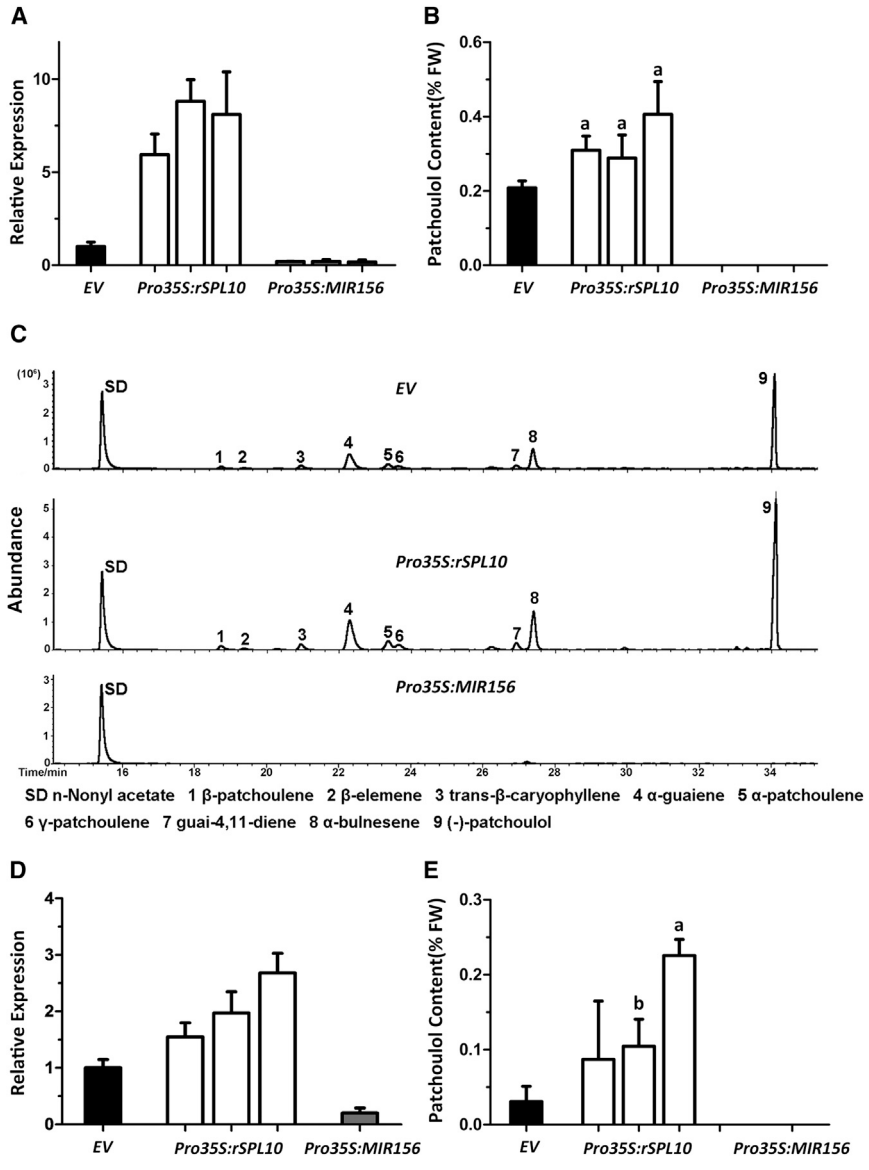

Figure 8. miR156-Targeted SPLs Regulate *PatPTS* Expression and Patchoulol Biosynthesis.

(A) Expression level of *PatPTS* in leaves of the 10-month-old *Empty Vector* (EV), *Pro35S:rSPL10*, and *Pro35S:MIR156* patchouli plants. The second fully expanded leaf was chosen. Error bars indicate the SD of three biological replicates.

(B) Content of (−)-patchoulol in leaves of the 10-month-old patchouli plants. The amount of (−)-patchoulol was first calculated by comparing with the internal standard and then dividing by the FW of the sample. Error bars indicate the SD of at least three biological replicates. Student's *t*-test, $^{a}P < 0.01$.

(C) GC–MS chromatogram of leaf extracts of the 10-month-old patchouli, showing sesquiterpene components. Nonyl acetate was included as an internal standard (SD). Note that sesquiterpenes were undetectable in *Pro35S:MIR156* leaves.

(D) Expression level of *PatPTS* in leaves of the 1-month-old regenerated patchouli plants. The second fully expanded leaf was analyzed. Error bars indicate the SD of three biological replicates.

(E) Contents of (−)-patchoulol in leaf of the 1-month-old patchouli plants. The amount of (−)-patchoulol was first calculated by comparing with the internal standard and then dividing by the FW of the sample. Error bars indicate the SD of three biological replicates. Student's *t*-test, $^{a}P < 0.01$ and $^{b}P < 0.05$.

multiple transcription factors control a single specialized metabolic pathway. Furthermore, it becomes an emerging phenomenon in plants that genes involved in the biosynthesis of a specific group of secondary metabolites tend to be clustered, which provides a cost-effective method for concerted regulation (Frey et al., 1997; Qi et al., 2004; Wilderman et al., 2004; Swaminathan et al., 2009; Falara et al., 2011; De Luca et al., 2012; Winzer et al., 2012; Mugford et al., 2013).

We previously reported that DELLA proteins, the negative regulator of the GA signaling pathway, interact with MYC2 and repress its activity on regulating *TPS21* and *TPS11* expression in flowers (Hong et al., 2012). A more recent report demonstrated that DELLAs interact with SPLs; this interaction disrupts the SPL-mediated activation on MADS box genes at the shoot apex and, in turn, delays flowering under both short-day and long-day conditions (Porri et al., 2012; Yu et al., 2012a). Although we found that the SPL regulation of *TPS21* expression is independent of MYC2, this does not preclude a possible interplay between DELLA, SPL, and MYC2, which may integrate both inner clues of plant development and external stimuli of environmental stresses into the orchestration of secondary metabolism in plants.

It has been reported in many plant species of different families that the terpenoid contents change during plant development. In addition to the species of Lamiaceae introduced above, lemongrass (*Cymbopogon flexuosus*) of the grass family (Poaceae) also shows age-dependent accumulation of terpenes (Singh et al., 1989; Lewinsohn et al., 1998). Furthermore, sesquiterpene levels were found to increase gradually along the internodes in an acropetal manner in *Solanum habrochaites* of the Solanaceae family (Besser et al., 2009). In the plant kingdom, miR156 is evolutionally conserved; the miR156 level declines and the target SPLs accumulate with plant age (Axtell and Bartel, 2005; Wang et al., 2009; Wu et al., 2009; Huijser and Schmid, 2011). It would be of great interest to examine whether the miR156-SPLs operate in a wide range of plant taxa in connecting plant development and aging to terpene biosynthesis. As demonstrated herein, overexpression of an *SPL* gene in patchouli not only increased patchouli oil content but also accelerated plant growth and the transition from juvenile to adult vegetative phases, thus providing a basis for the design of novel strategies to boost the essential oil yield in a shortened period of plant growth.

Sesquiterpenes	*Empty Vector*	*Pro35S:rSPL10*
β-Patchoulene	0.020 ± 0.007	0.028 ± 0.005[a]
β-Elemene	0.019 ± 0.007	0.024 ± 0.005
trans-β-Caryophyllene	0.037 ± 0.019	0.053 ± 0.011
α-Guaiene	0.266 ± 0.075	0.311 ± 0.055
α-Patchoulene	0.062 ± 0.021	0.078 ± 0.014
γ-Patchoulene	0.029 ± 0.009	0.037 ± 0.007[a]
Guai-4,11-diene	0.050 ± 0.017	0.062 ± 0.012
α-Bulnesene	0.279 ± 0.082	0.348 ± 0.057
(−)-Patchoulol	0.314 ± 0.099	0.429 ± 0.063[a]
Total	1.032 ± 0.368	1.369 ± 0.227[a]

Table 1. Contents (% Fresh Weight) of Sesquiterpene Constituents in Patchouli Leaf Essential Oil (Patchouli Oil).
The plants were transformed with *Empty Vector* (as control) or *Pro35S:rSPL10*. At least six 10-month-old plants of each line were analyzed. The amount of sesquiterpenes was first calculated by comparing with the internal standard and then dividing by the fresh weight of the sample. The nine sesquiterpene compounds listed are all present in the products of PatPTS (Deguerry et al., 2006; Wu et al., 2006). Values are mean ± SD. Student's *t*-test; [a]$P < 0.05$.

METHODS

Plant Materials and Constructs

A. thaliana (ecotype, Columbia-0) and *Nicotiana benthamiana* plants were grown at 22°C in long days (16 h light/8 h dark), and patchouli (*Pogostemon cablin*) was grown under similar conditions at 26°C. The cultivar of patchouli was from Firmenich.

The 1376-bp *Arabidopsis TPS21* promoter fragment was amplified using PrimeSTAR DNA Polymerase (Takara) and mutated by two-round PCR. The intact *TPS21* promoter was referred to as *INT*, which contained eight GTAC motifs. For the promoter mutants shown in Figure 5A, *mu1* was a deletion of six upstream GTAC motifs in cis1; *mu2* and *mu3* were the single mutant of the GTAC motif cis2 or cis3, which was changed to AAGA, respectively; *mu2+3* was the combination of *mu2* and *mu3* mutations; and *mu4* contained all mutations. For the GUS assay, these constructs were fused to the *GUS* reporter gene, introduced into *Arabidopsis*, and the GUS staining was performed as described (Jefferson et al., 1987). For the dual-LUC assay using *N. benthamiana* leaves, the promoters were fused to the firefly luciferase (*LUC*) reporter gene. The primers used in this investigation are listed in Supplemental Table 1.

Plant Treatments

For transient upregulation of *SPL9*, the 2-week-old *ProSPL9:rSPL9-GR Arabidopsis* plants were sprayed with either DEX or dimethyl sulfoxide (DMSO) (control), both at 10 μM. The rosette leaves were collected after a 5-h treatment. For transient downregulation of miR156-targeted *SPL* genes, the 4-week-old *ProAlcA:MIR156* bolting plants of *Arabidopsis* were sprayed with 5% ethanol or water (control), and the inflorescences were harvested after 6 h.

Patchouli Transformation

Plants of patchouli, line L002, were transformed. *Agrobacterium tumefaciens* EHA105 strains harboring *Pro35S:MIR156*, *Pro35S:rSPL10*, and *Empty Vector* were cultured overnight and resuspended in infection medium (1/2 MS medium, 45 g/l sucrose, 200 mM acetosyringone). Leaf dishes were then infected for 5 min and incubated at 24°C for 2 days on coculture medium (MS medium, 0.25 mg/l 6-benzyl aminopurine, 0.25 mg/l kinetin, 0.25 mg/l trans-zeatin, 0.25 mg/l indole-3-butyric acid, 100 mM acetosyringone), followed by incubation on selective differentiation medium (MS medium, 0.25 mg/l 6-benzyl aminopurine, 0.25 mg/l kinetin, 0.25 mg/l trans-zeatin, 0.25 mg/l indole-3-butyric acid, 500 mg/l carbenicillin, 100 mg/l kanamycin). Four weeks later, the greenish calli with adventitious shoot buds were transferred to selective elongation medium (MS medium, 0.1 mg/l 6-benzyl aminopurine, 300 mg/l carbenicillin, 100 mg/l kanamycin). Kanamycin-resistant shoots were rooted on the MS basal medium containing 200 mg/l carbenicillin and 50 mg/l kanamycin.

Expression Analysis

Total RNA was extracted from plant materials with Trizol reagent (Invitrogen). One microgram of total RNA, after treatment with DNase I, was used for cDNA synthesis with oligo(dT) primers and Moloney Murine Leukemia Virus Reverse Transcriptase (Invitrogen). Quantitative real-time RT-PCR was performed with SYBR-Green PCR Mastermix (Takara), and amplification was monitored in real time on a Mastercycler RealPlex^2 (Eppendorf). As internal reference, *β-TUBULIN2* was used for *Arabidopsis* and *Pat18S* (18S ribosomal RNA gene) for patchouli.

Volatile Analysis

The analysis was performed as previously described (Hong et al., 2012). In brief, approximately 0.5 g of inflorescence samples were detached from the 5-week-old *Arabidopsis*, which were incubated in μ-CTE (Micro-Chamber/Thermal Extractor) at 30°C for 1 h; the volatiles were collected by a Thermal Desorption Autosampler (Markes) with the Tenax TA (porous polymer) sorbent in a nitrogen gas flow. The adsorbed volatiles were desorbed and injected by a Thermal Desorber (TD100, Markes), followed by GC–MS (HP 6890/5973GC-MSD) analysis with nonyl acetate (10 ng, Aldrich) as internal standard. The GC–MS analysis was performed as described previously (Chen et al., 2003).

Patchouli Oil Extraction and GC–MS Analysis

Nine discs from three sequential fully expanded leaves (from the top) were picked with a hole punch (φ = 1 cm). After weighing, the materials were ground into powder with liquid nitrogen and resuspended with 1.5 ml of extraction buffer (hexane/ethyl acetate 85:15), which contained 20 ng/μl nonyl acetate as internal standard. The suspension was further sonicated for 20 min and then centrifuged at 5000 *g* for 5 min at room temperature. The supernatant was dehydrated with anhydrous Na_2SO_4 and used for GC–MS analysis. The column temperatures were programmed as follows: 80°C for 2 min, raised to 120°C at 3°C/min and held for 10 min, then raised to 170°C at 5°C/min and held for 10 min, then finally raised to 250°C at 20°C/min and held for 2 min. The injector temperature was 250°C. Helium was the carrier gas at 1.5 ml/min.

Electrophoretic Mobility Shift Assay

The open reading frame of *SPL9* was fused in-frame to the HIS-tag of the expression vector pET32a (Novagen), and the recombinant HIS-SPL9 proteins were affinity purified following the manual. For EMSA, the *TPS21* promoter segments, namely cis1, cis2, and cis3, were labeled with Cy5 on both ends. The DNA fragment and the purified proteins were incubated at 25°C for 30 min in the buffer containing 1 mg/ml poly(dI–dC) (Roche, USA), 20 mM Tris-base (pH 7.5), 1 mM dithiothreitol, 10 mM $MgCl_2$, 0.5 mg/ml calf bovine serum albumin, and 5% glycerol, and then separated by 5% native polyacrylamide gel electrophoresis in 0.5× TBE buffer at 10 V/cm and 4°C. The fluorescence was detected with a Fujifilm FLA-9000 image scanner.

Chromatin Immunoprecipitation Assay

Approximately 5 g of flower buds of 4-week-old *ProSPL9:GFP-rSPL9* and the wild-type plants were harvested. After fixation, the materials were washed and ground into powder in liquid nitrogen and resuspended in extraction buffer (0.4 M sucrose, 10 mM Tris–HCl [pH 8.0], 10 mM $MgCl_2$, 5 mM mercaptoethanol, 0.1 mM PMSF, and 1× protease inhibitor)

and lysis buffer (50 mM HEPES [pH 7.5], 150 mM NaCl, 1 mM EDTA, 1% Triton X-100, 0.1% deoxycholate sodium, and 0.1% SDS) in turn, followed by sonification (output 3, 6 × 10 s). One-third of the crude chromatin extracts was saved as input control and the other two-thirds were treated with anti-GFP or anti-HA (Abmart) antibodies, separately. After precipitation, the resulting DNA samples were purified with a PCR purification kit (Qiagen). The abundance of the DNA fragments was analyzed by qRT-PCR with *β-TUBULIN2* promoter as a reference, as described (Yu et al., 2010). The relative enrichment of each fragment was calculated first by normalizing the value for anti-GFP against the value for anti-HA and then comparing the result for *ProSPL9:GFP-rSPL9* with that of the wild-type plants.

Dual-Luciferase Assay of Transient Regulation

The assay was performed following a published protocol (Liu et al., 2008). In brief, the wild-type and the mutant versions of the *TPS21* promoter were inserted into *pGreen-LUC* plasmid driving the firefly luciferase reporter gene with the Renilla (REN) luciferase controlled by the constitutive 35S promoter on the same plasmid as a reference to normalize infection efficiency. The constructs were then transferred into *Agrobacterium* (strain GV3101) with the helper plasmid, *pSoup-P19*, which also encodes a repressor of cosuppression. The transformed *Agrobacterium* cells were mixed with the *Agrobacterium* strains containing the effector *Pro35S:rSPL9* or *Empty Vector* in a ratio of 1:4.

Transient transformation was conducted by infiltration of the *Agrobacterium* mixture into the abaxial side of *N. benthamiana* leaves using a syringe. After culturing for 3 days, the infected area was collected for total protein extraction. The supernatant of the total protein was reacted with commercial dual-LUC reaction reagents (Promega, E1910) and the fluorescent values of LUC and REN were detected successively with a luminometer (BG-1, GEM Biomedical). The value of LUC was first compared with that of REN and then the ratio (LUC/REN) cotransformed with *Pro35S:rSPL9* was normalized against the ratio cotransformed with *Empty Vector*.

ACCESSION NUMBERS

Arabidopsis Genome Initiative gene identifiers are as follows: *SPL3* (At2g33810), *SPL9* (At2g42200), *SPL10* (At1g27370), *MIR156f* (At5g26147), *TPS03* (At4g16740), *TPS11* (At5g44630), *TPS14* (At1g61680), *TPS17* (At3g14490), *TPS18* (At3g14520), *TPS21* (At5g23960), *TPS24* (At3g25810), *HMGR1* (At1g76490), *HMGR2* (At2g17370), *FPS1* (At4g17190), *FPS2* (At5g47770), and *β-TUBULIN2* (At5g62690). Mutants and transgenic plants of *spl9* (SAIL_150_B05), *myc2-2* (SALK_083483), *Pro35S:MIR156*, *Pro35S:MIM156*, *Pro35S:rSPL3*, *ProSPL9:rSPL9*, *Pro35S:rSPL10*, *ProSPL9:rSPL9-GR*, *ProAlcA:MIR156*, *ProSPL9:GFP-rSPL9*, and *ProTPS21mu2:GUS* (renamed as *ProTPS21 E-box mu2:GUS*) were as described previously (Wang et al., 2009; Wu et al., 2009; Hong et al., 2012).

Patchouli genes mentioned in this article can be accessed as follows: *PatTpsA* (AY508726), *PatTpsBF2* (AY508727), *PatTpsCF2* (AY508728), *PatTpsB15* (AY508729), *PatPTS* (AY508730), *Pat18S* (FJ980282).

SUPPLEMENTAL INFORMATION

Supplemental Information is available at *Molecular Plant Online*.

FUNDING

This research was supported by the Strategic Priority Research Program of the Chinese Academy of Sciences (XDB11030000), State Key Basic Research Program of China (2013CB127000), the Special Fund for Shanghai Landscaping Administration Bureau Program (F112418), and the National Natural Science Foundation of China (31300255).

ACKNOWLEDGMENTS

We thank the ABRC for *Arabidopsis* T-DNA insertion lines, Jia-Wei Wang, Gao-Jie Hong, and Xue-Yi Xue for sharing materials and helpful discussions, and Wen-Li Hu for the GC–MS analysis. All the authors have no conflicts to declare.

Received: June 8, 2014
Accepted: October 25, 2014
Published: October 29, 2014

REFERENCES

Aharoni, A., Giri, A.P., Deuerlein, S., Griepink, F., de Kogel, W.J., Verstappen, F.W., Verhoeven, H.A., Jongsma, M.A., Schwab, W., and Bouwmeester, H.J. (2003). Terpenoid metabolism in wild-type and transgenic Arabidopsis plants. Plant Cell **15**:2866–2884.

Aubourg, S., Lecharny, A., and Bohlmann, J. (2002). Genomic analysis of the terpenoid synthase (AtTPS) gene family of Arabidopsis thaliana. Mol. Genet. Genomics **267**:730–745.

Axtell, M.J., and Bartel, D.P. (2005). Antiquity of microRNAs and their targets in land plants. Plant Cell **17**:1658–1673.

Balbi, V., and Devoto, A. (2008). Jasmonate signalling network in Arabidopsis thaliana: crucial regulatory nodes and new physiological scenarios. New Phytol. **177**:301–318.

Besser, K., Harper, A., Welsby, N., Schauvinhold, I., Slocombe, S., Li, Y., Dixon, R.A., and Broun, P. (2009). Divergent regulation of terpenoid metabolism in the trichomes of wild and cultivated tomato species. Plant Physiol. **149**:499–514.

Birkenbihl, R.P., Jach, G., Saedler, H., and Huijser, P. (2005). Functional dissection of the plant-specific SBP-domain: overlap of the DNA-binding and nuclear localization domains. J. Mol. Biol. **352**:585–596.

Bohlmann, J., Meyer-Gauen, G., and Croteau, R. (1998). Plant terpenoid synthases: molecular biology and phylogenetic analysis. Proc. Natl. Acad. Sci. U S A **95**:4126–4133.

Bouwmeester, H.J., Gershenzon, J., Konings, M.C., and Croteau, R. (1998). Biosynthesis of the monoterpenes limonene and carvone in the fruit of caraway. I. Demonstration of enzyme activities and their changes with development. Plant Physiol. **117**:901–912.

Buré, C.M., and Sellier, N.M. (2004). Analysis of the essential oil of Indonesian patchouli (Pogostemon cablin Benth.) using GC/MS (EI/CI). J. Essent. Oil Res. **16**:17–19.

Chen, F., Tholl, D., D'Auria, J.C., Farooq, A., Pichersky, E., and Gershenzon, J. (2003). Biosynthesis and emission of terpenoid volatiles from Arabidopsis flowers. Plant Cell **15**:481–494.

Christianson, D.W. (2008). Unearthing the roots of the terpenome. Curr. Opin. Chem. Biol. **12**:141–150.

Cunillera, N., Boronat, A., and Ferrer, A. (2000). Spatial and temporal patterns of GUS expression directed by 5' regions of the Arabidopsis thaliana farnesyl diphosphate synthase genes FPS1 and FPS2. Plant Mol. Biol. **44**:747–758.

Degenhardt, J., Kollner, T.G., and Gershenzon, J. (2009). Monoterpene and sesquiterpene synthases and the origin of terpene skeletal diversity in plants. Phytochemistry **70**:1621–1637.

Deguerry, F., Pastore, L., Wu, S., Clark, A., Chappell, J., and Schalk, M. (2006). The diverse sesquiterpene profile of patchouli, Pogostemon cablin, is correlated with a limited number of sesquiterpene synthases. Arch. Biochem. Biophys. **454**:123–136.

De Luca, V., Salim, V., Atsumi, S.M., and Yu, F. (2012). Mining the biodiversity of plants: a revolution in the making. Science **336**:1658–1661.

Dudareva, N., Martin, D., Kish, C.M., Kolosova, N., Gorenstein, N., Faldt, J., Miller, B., and Bohlmann, J. (2003). (E)-beta-ocimene and myrcene synthase genes of floral scent biosynthesis in snapdragon: function and expression of three terpene synthase genes of a new terpene synthase subfamily. Plant Cell **15**:1227–1241.

Dudareva, N., Pichersky, E., and Gershenzon, J. (2004). Biochemistry of plant volatiles. Plant Physiol. **135**:1893–1902.

Engelberth, J., Alborn, H.T., Schmelz, E.A., and Tumlinson, J.H. (2004). Airborne signals prime plants against insect herbivore attack. Proc. Natl. Acad. Sci. U S A **101**:1781–1785.

Enjuto, M., Balcells, L., Campos, N., Caelles, C., Arro, M., and Boronat, A. (1994). Arabidopsis thaliana contains two differentially expressed 3-hydroxy-3-methylglutaryl-CoA reductase genes, which encode microsomal forms of the enzyme. Proc. Natl. Acad. Sci. U S A **91**:927–931.

Facchini, P.J., and De Luca, V. (1995). Phloem-specific expression of tyrosine/dopa decarboxylase genes and the biosynthesis of isoquinoline alkaloids in opium poppy. Plant Cell **7**:1811–1821.

Falara, V., Akhtar, T.A., Nguyen, T.T., Spyropoulou, E.A., Bleeker, P.M., Schauvinhold, I., Matsuba, Y., Bonini, M.E., Schilmiller, A.L., Last, R.L., et al. (2011). The tomato terpene synthase gene family. Plant Physiol. **157**:770–789.

Falara, V., and Pichersky, E. (2012). Plant volatiles and other specialized metabolites: synthesis, storage, emission, and function. In Secretions and Exudates in Biological Systems, Signaling and Communication in Plants, *Vol. 12*, pp. 109–123.

Franco-Zorrilla, J.M., Valli, A., Todesco, M., Mateos, I., Puga, M.I., Rubio-Somoza, I., Leyva, A., Weigel, D., Garcia, J.A., and Paz-Ares, J. (2007). Target mimicry provides a new mechanism for regulation of microRNA activity. Nat. Genet. **39**:1033–1037.

Frey, M., Chomet, P., Glawischnig, E., Stettner, C., Grun, S., Winklmair, A., Eisenreich, W., Bacher, A., Meeley, R.B., Briggs, S.P., et al. (1997). Analysis of a chemical plant defense mechanism in grasses. Science **277**:696–699.

Gershenzon, J., McConkey, M.E., and Croteau, R.B. (2000). Regulation of monoterpene accumulation in leaves of peppermint. Plant Physiol. **122**:205–214.

Goff, S.A., and Klee, H.J. (2006). Plant volatile compounds: sensory cues for health and nutritional value? Science **311**:815–819.

Gou, J.Y., Felippes, F.F., Liu, C.J., Weigel, D., and Wang, J.W. (2011). Negative regulation of anthocyanin biosynthesis in Arabidopsis by a miR156-targeted SPL transcription factor. Plant Cell **23**:1512–1522.

Guo, A.Y., Zhu, Q.H., Gu, X., Ge, S., Yang, J., and Luo, J. (2008). Genome-wide identification and evolutionary analysis of the plant specific SBP-box transcription factor family. Gene **418**:1–8.

Haubold, B., Kroymann, J., Ratzka, A., Mitchell-Olds, T., and Wiehe, T. (2002). Recombination and gene conversion in a 170-kb genomic region of Arabidopsis thaliana. Genetics **161**:1269–1278.

Hoffmann, M.H., Bremer, M., Schneider, K., Burger, F., Stolle, E., and Moritz, G. (2003). Flower visitors in a natural population of Arabidopsis thaliana. Plant Biol. **5**:491–494.

Hong, G.J., Xue, X.Y., Mao, Y.B., Wang, L.J., and Chen, X.Y. (2012). Arabidopsis MYC2 interacts with DELLA proteins in regulating sesquiterpene synthase gene expression. Plant Cell **24**:2635–2648.

Huang, M., Sanchez-Moreiras, A.M., Abel, C., Sohrabi, R., Lee, S., Gershenzon, J., and Tholl, D. (2012). The major volatile organic compound emitted from Arabidopsis thaliana flowers, the sesquiterpene (E)-beta-caryophyllene, is a defense against a bacterial pathogen. New Phytol. **193**:997–1008.

Huijser, P., and Schmid, M. (2011). The control of developmental phase transitions in plants. Development **138**:4117–4129.

Jefferson, R.A., Kavanagh, T.A., and Bevan, M.W. (1987). GUS fusions: beta-glucuronidase as a sensitive and versatile gene fusion marker in higher plants. EMBO J. **6**:3901–3907.

Kessler, A., and Baldwin, I.T. (2001). Defensive function of herbivore-induced plant volatile emissions in nature. Science **291**:2141–2144.

Klein, J., Saedler, H., and Huijser, P. (1996). A new family of DNA binding proteins includes putative transcriptional regulators of the Antirrhinum majus floral meristem identity gene SQUAMOSA. Mol. Gen. Genet. **250**:7–16.

Kropat, J., Tottey, S., Birkenbihl, R.P., Depege, N., Huijser, P., and Merchant, S. (2005). A regulator of nutritional copper signaling in Chlamydomonas is an SBP domain protein that recognizes the GTAC core of copper response element. Proc. Natl. Acad. Sci. U S A **102**:18730–18735.

Kuittinen, H., and Aguade, M. (2000). Nucleotide variation at the CHALCONE ISOMERASE locus in Arabidopsis thaliana. Genetics **155**: 863–872.

Lewinsohn, E., Dudai, N., Tadmor, Y., Katzir, I., Ravid, U., Putievsky, E., and Joel, D.M. (1998). Histochemical localization of citral accumulation in lemongrass leaves (*Cymbopogon citrates* (DC.) Stapf., Poaceae). Ann. Bot. **81**:35–39.

Li, J.W., and Vederas, J.C. (2009). Drug discovery and natural products: end of an era or an endless frontier? Science **325**:161–165.

Liang, X., Nazarenus, T.J., and Stone, J.M. (2008). Identification of a consensus DNA-binding site for the Arabidopsis thaliana SBP domain transcription factor, AtSPL14, and binding kinetics by surface plasmon resonance. Biochemistry **47**:3645–3653.

Liu, H., Yu, X., Li, K., Klejnot, J., Yang, H., Lisiero, D., and Lin, C. (2008). Photoexcited CRY2 interacts with CIB1 to regulate transcription and floral initiation in Arabidopsis. Science **322**:1535–1539.

Ma, D., Pu, G., Lei, C., Ma, L., Wang, H., Guo, Y., Chen, J., Du, Z., Li, G., Ye, H., et al. (2009). Isolation and characterization of AaWRKY1, an Artemisia annua transcription factor that regulates the amorpha-4,11-diene synthase gene, a key gene of artemisinin biosynthesis. Plant Cell Physiol. **50**:2146–2161.

Maffei, M.E., Gertsch, J., and Appendino, G. (2011). Plant volatiles: production, function and pharmacology. Nat. Prod. Rep. **28**:1359–1380.

Mandaokar, A., Thines, B., Shin, B., Lange, B.M., Choi, G., Koo, Y.J., Yoo, Y.J., Choi, Y.D., and Browse, J. (2006). Transcriptional regulators of stamen development in Arabidopsis identified by transcriptional profiling. Plant J. **46**:984–1008.

Memelink, J., Verpoorte, R., and Kijne, J.W. (2001). ORCAnization of jasmonate-responsive gene expression in alkaloid metabolism. Trends Plant Sci. **6**:212–219.

Mugford, S.T., Louveau, T., Melton, R., Qi, X., Bakht, S., Hill, L., Tsurushima, T., Honkanen, S., Rosser, S.J., Lomonossoff, G.P., et al. (2013). Modularity of plant metabolic gene clusters: a trio of linked genes that are collectively required for acylation of triterpenes in oat. Plant Cell **25**:1078–1092.

Newman, J.D., and Chappell, J. (1999). Isoprenoid biosynthesis in plants: carbon partitioning within the cytoplasmic pathway. Crit. Rev. Biochem. Mol. Biol. **34**:95–106.

Nodine, M.D., and Bartel, D.P. (2010). MicroRNAs prevent precocious gene expression and enable pattern formation during plant embryogenesis. Genes Dev. **24**:2678–2692.

Pichersky, E., and Gang, D.R. (2000). Genetics and biochemistry of secondary metabolites in plants: an evolutionary perspective. Trends Plant Sci. **5**:439–445.

Pichersky, E., and Gershenzon, J. (2002). The formation and function of plant volatiles: perfumes for pollinator attraction and defense. Curr. Opin. Plant Biol. **5**:237–243.

Porri, A., Torti, S., Romera-Branchat, M., and Coupland, G. (2012). Spatially distinct regulatory roles for gibberellins in the promotion of flowering of Arabidopsis under long photoperiods. Development **139**:2198–2209.

Qi, X., Bakht, S., Leggett, M., Maxwell, C., Melton, R., and Osbourn, A. (2004). A gene cluster for secondary metabolism in oat: implications for the evolution of metabolic diversity in plants. Proc. Natl. Acad. Sci. U S A **101**:8233–8238.

Reeves, P.H., Ellis, C.M., Ploense, S.E., Wu, M.F., Yadav, V., Tholl, D., Chetelat, A., Haupt, I., Kennerley, B.J., Hodgens, C., et al. (2012). A regulatory network for coordinated flower maturation. PLoS Genet. **8**:e1002506.

Schwarz, S., Grande, A.V., Bujdoso, N., Saedler, H., and Huijser, P. (2008). The microRNA regulated SBP-box genes SPL9 and SPL15 control shoot maturation in Arabidopsis. Plant Mol. Biol. **67**:183–195.

Shikata, M., Koyama, T., Mitsuda, N., and Ohme-Takagi, M. (2009). Arabidopsis SBP-box genes SPL10, SPL11 and SPL2 control morphological change in association with shoot maturation in the reproductive phase. Plant Cell Physiol. **50**:2133–2145.

Shoji, T., and Hashimoto, T. (2011). Tobacco MYC2 regulates jasmonate-inducible nicotine biosynthesis genes directly and by way of the NIC2-locus ERF genes. Plant Cell Physiol. **52**:1117–1130.

Singh, N., Luthra, R., and Sangwan, R.S. (1989). Effect of leaf position and age on the essential oil quantity and quality in lemongrass (*Cymbopogon flexuosus*). Planta Med. **55** (3):254–256.

Stahl, E.A., Dwyer, G., Mauricio, R., Kreitman, M., and Bergelson, J. (1999). Dynamics of disease resistance polymorphism at the Rpm1 locus of Arabidopsis. Nature **400**:667–671.

Swaminathan, S., Morrone, D., Wang, Q., Fulton, D.B., and Peters, R.J. (2009). CYP76M7 is an ent-cassadiene C11alpha-hydroxylase defining a second multifunctional diterpenoid biosynthetic gene cluster in rice. Plant Cell **21**:3315–3325.

Tholl, D., Chen, F., Petri, J., Gershenzon, J., and Pichersky, E. (2005). Two sesquiterpene synthases are responsible for the complex mixture of sesquiterpenes emitted from Arabidopsis flowers. Plant J. **42**: 757–771.

Tholl, D., and Lee, S. (2011). Terpene specialized metabolism in Arabidopsis thaliana. Arabidopsis Book **9**:e0143.

Turner, G.W., Gershenzon, J., and Croteau, R.B. (2000). Distribution of peltate glandular trichomes on developing leaves of peppermint. Plant Physiol. **124**:655–664.

Usami, T., Horiguchi, G., Yano, S., and Tsukaya, H. (2009). The more and smaller cells mutants of Arabidopsis thaliana identify novel roles for SQUAMOSA PROMOTER BINDING PROTEIN-LIKE genes in the control of heteroblasty. Development **136**:955–964.

Wang, J.W., Czech, B., and Weigel, D. (2009). miR156-regulated SPL transcription factors define an endogenous flowering pathway in Arabidopsis thaliana. Cell **138**:738–749.

Wang, J.W., Schwab, R., Czech, B., Mica, E., and Weigel, D. (2008). Dual effects of miR156-targeted SPL genes and CYP78A5/KLUH on plastochron length and organ size in Arabidopsis thaliana. Plant Cell **20**:1231–1243.

Wilderman, P.R., Xu, M., Jin, Y., Coates, R.M., and Peters, R.J. (2004). Identification of syn-pimara-7,15-diene synthase reveals functional clustering of terpene synthases involved in rice phytoalexin/ allelochemical biosynthesis. Plant Physiol. **135**:2098–2105.

Winzer, T., Gazda, V., He, Z., Kaminski, F., Kern, M., Larson, T.R., Li, Y., Meade, F., Teodor, R., Vaistij, F.E., et al. (2012). A Papaver somniferum 10-gene cluster for synthesis of the anticancer alkaloid noscapine. Science **336**:1704–1708.

Wu, G., Park, M.Y., Conway, S.R., Wang, J.W., Weigel, D., and Poethig, R.S. (2009). The sequential action of miR156 and miR172 regulates developmental timing in Arabidopsis. Cell **138**:750–759.

Wu, S., Schalk, M., Clark, A., Miles, R.B., Coates, R., and Chappell, J. (2006). Redirection of cytosolic or plastidic isoprenoid precursors elevates terpene production in plants. Nat. Biotechnol. **24**:1441–1447.

Xing, S., Salinas, M., Garcia-Molina, A., Hohmann, S., Berndtgen, R., and Huijser, P. (2013). SPL8 and miR156-targeted SPL genes redundantly regulate Arabidopsis gynoecium differential patterning. Plant J. **75**:566–577.

Xing, S., Salinas, M., Hohmann, S., Berndtgen, R., and Huijser, P. (2010). miR156-targeted and nontargeted SBP-box transcription factors act in concert to secure male fertility in Arabidopsis. Plant Cell **22**:3935–3950.

Yamaguchi, A., Wu, M.F., Yang, L., Wu, G., Poethig, R.S., and Wagner, D. (2009). The microRNA-regulated SBP-Box transcription factor SPL3 is a direct upstream activator of LEAFY, FRUITFULL, and APETALA1. Dev. Cell **17**:268–278.

Yu, N., Cai, W.J., Wang, S., Shan, C.M., Wang, L.J., and Chen, X.Y. (2010). Temporal control of trichome distribution by microRNA156-targeted SPL genes in Arabidopsis thaliana. Plant Cell **22**:2322–2335.

Yu, S., Galvao, V.C., Zhang, Y.C., Horrer, D., Zhang, T.Q., Hao, Y.H., Feng, Y.Q., Wang, S., Schmid, M., and Wang, J.W. (2012a). Gibberellin regulates the Arabidopsis floral transition through miR156-targeted SQUAMOSA PROMOTER BINDING-LIKE transcription factors. Plant Cell **24**:3320–3332.

Yu, Z.X., Li, J.X., Yang, C.Q., Hu, W.L., Wang, L.J., and Chen, X.Y. (2012b). The jasmonate-responsive AP2/ERF transcription factors AaERF1 and AaERF2 positively regulate artemisinin biosynthesis in Artemisia annua L. Mol. Plant **5**:353–365.

Zaim, M., Ali, A., Joseph, J., and Khan, F. (2013). Serological and molecular studies of a novel virus isolate causing yellow mosaic of Patchouli [Pogostemon cablin (Blanco) Benth]. PLoS One **8**:e83790.

Zhang, H.B., Bokowiec, M.T., Rushton, P.J., Han, S.C., and Timko, M.P. (2012). Tobacco transcription factors NtMYC2a and NtMYC2b form nuclear complexes with the NtJAZ1 repressor and regulate multiple jasmonate-inducible steps in nicotine biosynthesis. Mol. Plant **5**:73–84.